Molecular Dynamics Simulations of Ferrocene-Terminated Self-Assembled Monolayers

F. Goujon,[†] C. Bonal,*[,†] B. Limoges,[‡] and P. Malfreyt[†]

Laboratoire Thermodynamique et Interactions Moléculaires, UMR CNRS 6272, Université Blaise Pascal, 63177 Aubière Cedex, France, and Laboratoire d'Electrochimie Moléculaire, UMR CNRS 7591, Université Paris Diderot, 15 rue Jean-Antoine de Baïf, 75205 Paris Cedex 13, France

Received: December 3, 2009; Revised Manuscript Received: March 31, 2010

The present work describes our studies of the $Fc(CH_2)_{12}S$-/$C_{10}S$-Au monolayers to provide a more detailed molecular description. Molecular dynamics simulations of these mixed monolayers are carried out in conditions close to the electrochemical ones. For this purpose, a supporting electrolyte is added ($NaClO_4$ 1 M) and the electron transfer process is modeled through molecular simulations of ferrocene both in its neutral (initial state) and oxidized form (final state). The heterogeneity of the surface, that is, "clustered " or "isolated" ferrocene moieties, has been considered for the ferrocenylalkylthiolates using the same grafting densities. The structural properties (density profiles and angular distributions) are described in terms of redox induced orientation changes by comparison between the initial and final states. It is established that this orientation change due to the oxidation of the ferrocene to the ferrocenium is mainly observed in the random system, and it is less pronounced in the cluster system. Finally, the energy contributions underline the role played by the supporting electrolyte.

Introduction

Self-assembled monolayers (SAMs) are well-organized arrays of organic molecules that form spontaneously from the adsorption of molecular constituents on a suitable substrate. Because of their broad range of applications in chemical, electronic, and biotechnological fields,[1−7] there has been a continuing interest in a comprehensive study of their structure and properties.[8−11] Alkanethiol-based SAMs on the Au surface are commonly used as a model system for studying specific structural features of monomolecular films. They are also used to determine how chemical alterations in the backbone chain and/or the terminal group affect the structure of the formed film. In addition, the use of alkanethiols containing terminal redox-active groups opens up the possibility of obtaining more information about SAM structure and investigating mechanisms of electron transfer from the molecular layer to the electrode.

The ferrocene-terminated self-assembled monolayer (Fc-SAM) is probably the most studied of all electrochemically active SAMs. Starting from the pioneering work of Chidsey,[12] these SAMs have been extensively used as convenient, robust, and well-reproducible surface self-assemblies. The thermodynamic characteristics of these electroactive sites are strongly affected by the nature of the environment where they are placed. A large number of studies described how the complexities in the Fc-SAM electrochemical systems[12−31] are in fact attributable to the local environment of the ferrocenylalkylthiolate chain in the Fc-SAM.[32,33] This system presents a quasi-ideal electrochemistry signature when the surface coverage of ferrocenylalkylthiolates is low and diluted by nonelectroactive alkanethiolates. However, at relatively high surface coverage of ferrocenylalkylthiolates, cyclic voltammetric studies have reported nonideal electrochemical behavior.[13−15,20−31,34] Two oxidation peaks, whose shapes, positions, and relative sizes are dependent on ferrocene mole fraction in solution were frequently observed.[20,22,26,29−31,34] Several assumptions were proposed to explain these phenomena such as structural disorder in the SAM due to steric crowding of Fc groups,[13,21,35] double-layer effects,[26,34−38] different structural orders of the monolayer,[14,15] or differences due to the Au polycrystalline structure.[39] Recent studies also suggest that this behavior arises from a "spatial inhomogeneity" in the SAM with Fc groups that are isolated from other Fc molecules (by alkylthiolates, for example) and Fc groups that are proximal to one other (in "clustered" state).[25,32,40,41]

Recently, we have developed a methodology to study heterogeneous systems with a finite length in the third dimension[42−45] by molecular simulations. From a computational viewpoint, the presence of the surface creates a nonuniformity of the local density along the direction normal to the surface and gives rise to important issues concerning the truncation procedures and the methodology used to take into account the Coulombic interactions. This methodology was applied[46] to obtain a prerequisite work of $Fc(CH_2)_{12}S$-/$C_{10}S$-Au monolayers in water. Five reference systems were simulated using different grafting densities for ferrocenylalkylthiolates to explore the possible inhomogeneity of the neutral ferrocene moieties within the layer. The computed quantities (density profiles, angular distributions, positions of atoms, and energetic description) have improved the understanding of the ordering tendency of the chains. By connecting the structural features and the energy contributions deduced from molecular simulations, the relative contributions from isolated and clustered neutral Fc moieties were described. Now, the next step toward a better insight of these electrochemical systems consists in changing the ferrocene (neutral form) to ferrocenium (cationic form Fc^+).

The present work is devoted to the $Fc(CH_2)_{12}S$-/$C_{10}S$-Au monolayers to provide a more detailed molecular description in conditions close to the electrochemical experiments. For this purpose, a supporting electrolyte much more concentrated than the electroactive species is added ($NaClO_4$, 1 M). The oxidation

* To whom correspondence should be addressed. E-mail: Christine.Bonal@univ-bpclermont.fr.
[†] LTIM, UMR CNRS 6272.
[‡] UMR CNRS 7591.

10.1021/jp911467x
Published on Web 04/22/2010

of the neutral ferrocene involves coupled electron-transfer and also anion-pairing reactions. It is well-known that, when redox reactions of the terminal groups create or annihilate charges at the monolayer/solution interface, the formation or dissociation of ion pairs may occur.[14,15,27,47−51] Such a process is frequently accompanied by the orientation/structural change of the alkanethiol molecules (redox-induced orientation change[14,15,24,49,52]). The nature and the concentration of the anion in the bulk electrolyte play a significant role in the overall oxidation process. The ion pairing directly influences the stability of the Fc-terminated monolayer. There is extensive experimental evidence indicating an ion-pairing ability of the oxidized surface-bound ferrocinium ion (Fc^+) with anions, especially with perchlorate.[35,50,53−56] The majority of researchers employ perchlorate-dominated buffers in their experiments. In fact, experimentalists use perchlorate because it seems very difficult to achieve reversible recycling of Fc/Fc^+ in the presence of most other anions because they attack Fc^+ in a nucleophilic manner and decompose the Fc. It is an entirely practical origin, as perchlorate has very low nucleophility. Moreover, perchlorate yields the largest effective ion-pair formation constant.[54] This means that this electrolyte anion probably has a strong effect on the thermodynamics of the ferrocene interfacial redox reaction. This should allow us to observe more significant differences between the neutral (initial state) and oxidized form (final state). As a consequence, we take the route of using this anion in our MD simulation.

To take into account the heterogeneity of the surface in this work ("clustered" or "isolated" states of Fc molecules) the electron-transfer process is modeled by molecular simulations of Fc both in its neutral and oxidized form in two reference systems. These latters used the same grafting densities for the ferrocenylalkylthiolates but different surface organizations for the molecules (cluster and random systems). We decided to model the two states separetely to obtain pronounced differences between these two states. In the case of the clustered system, the alkyl and alkylferrocene chains can be considered as molecules phase separated, whereas in the isolated system the alkylferrocene chains are diluted by the alkyl chains. For the latter system, each molecule experiences almost the same environment. They can be treated as isolated species. Since MD simulations are highly successful in capturing the structural properties of SAMs, we propose to explore the possibility of redox-induced orientation change by investigating the density profiles and the angular distributions. Finally, we complete the molecular description by the calculation of the energetic properties of these monolayers.

The outline of this work is as follows. In the section concerning the experimental methods, we give the details of the computational procedures and we present the potential model. In this part, we also describe the two systems of $Fc(CH_2)_{12}S$-/$C_{10}S$-Au monolayers used to model dilute and clusterized Fc systems. In the next section, we discuss the results of the stuctural and energetical properties. Finally, in the last section we draw the main conclusions from this work.

Computational Procedures

Model. The system consists of five layers of a Au(111) surface grafted with n-C_{10} alkylthiolate ($C_{10}H_{21}S$) and n-C_{12} ferrocenyalkylthiolate ($C_{22}H_{33}FeS$) molecules. We used the all-atom (AA) version of the Cornell force field AMBER[57] for grafted molecules. The Au parameters were taken from the work of Ayappa and co-workers.[58] The ferrocene part was modeled using the parameters described by Canongia Lopes et al.[59] The general potential function is of the form

$$U = \sum_{\text{bonds}} k_b(r - r_o)^2 + \sum_{\text{angles}} k_\theta(\theta - \theta_o)^2 + \sum_{\text{dihedrals}} k_\phi[1 + \cos(l\phi + \delta)] + \sum_{i=1}^{N-1}\sum_{j=i+1}^{N}\left\{4\varepsilon_{ij}\left[\left(\frac{\sigma_{ij}}{r_{ij}}\right)^{12} - \left(\frac{\sigma_{ij}}{r_{ij}}\right)^{6}\right] + \sum_{l}^{\infty}{}' \frac{q_i q_j}{|\mathbf{r_{ij}} + \mathbf{n}L|}\right\} \quad (1)$$

where k_b, k_θ, and k_ϕ are the force constants for deformation of bonds, angles, and dihedrals, respectively. The equilibrium values of bond distances and valence angles correspond to r_o and θ_o, respectively. In the dihedral angle term, l is the periodicity, and δ is the phase factor. The C−H covalent bonds were kept of fixed length by using the SHAKE algorithm.[60] The intermolecular and intramolecular interactions consist of a van der Waals repulsion−dispersion term calculated using the Lennard-Jones (6−12) potential, represented by the penultimate term in eq 1. In the AMBER force field, the nonbonded interactions between atoms separated by exactly three bonds (1−4 van der Waals interactions) are reduced by a factor of 0.5.[57] The Lennard-Jones potential parameters for the interactions between unlike atoms were calculated by using the Lorentz−Berthelot mixing rules (quadratic and arithmetic rules for ε_{ij} and σ_{ij} parameters, respectively). The water molecules were represented with the TIP4P/2005 model.[61] As the system is nonperiodic in the direction normal to the surface (z-axis), the simulation cell is closed by an additional gold layer. The distance between the two inner surfaces was chosen to be 80 Å, which is large enough for the water molecules in the middle of the cell to have a bulk behavior.[42] The simulation cell was then elongated in the z direction so that a sufficiently large empty space is left between the periodic images to dampen out the interslab interactions. A supporting electrolyte $NaClO_4$ is added in the water phase. The Na^+ and ClO_4^- ions are represented with the model described by Wu et al.[62]

Long-Range Coulombic Interaction. The last term in eq 1 corresponds to the electrostatic energy (U_{ELEC}) of the system. Considering N molecules in a volume $V = L_x L_y L_z$ with center of mass $\mathbf{r}_i$, each molecule contains n_i charges q_{ia} at position $\mathbf{r}_{ia}$. The electrostatics interactions handled with the Ewald sum method[63,64] in a box with orthogonal axis are given by the following contributions

$$U_{\text{ELEC}} = \frac{1}{2\varepsilon_o V}\sum_{k\neq 0} Q(h)\, S(\mathbf{h})\, S(-\mathbf{h}) + \frac{1}{8\pi\varepsilon_o}\sum_i\sum_a\sum_{j\neq i} q_{ia}\sum_b q_{jb}\,\text{erfc}(\alpha r_{iajb})/r_{iajb} - \frac{\alpha}{4\pi^{3/2}\varepsilon_o}\sum_i\sum_a q_{ia}{}^2 - \frac{1}{8\pi\varepsilon_o}\sum_i\sum_a\sum_{b\neq a}\frac{q_{ia}q_{ib}}{r_{iaib}}\,\text{erf}(\alpha r_{iaib}) + \frac{1}{2\varepsilon_o V}M_z{}^2 \quad (2)$$

where $\text{erfc}(x)$ is the complementary error function and $\text{erf}(x)$ is the error function. α is chosen so that only pair interactions in the central cell need to be considered in evaluating the second term in eq 2. Note that the overall charge of the simulation cell

must be zero. In the last term of eq 2, M_z is the net dipole moment of the simulation cell given by $\sum_{i=1}^{N} q_i \mathbf{r}_i$. This contribution is the correction term of Yeh and Berkowitz[65] which results from the plane-wise summation method proposed by Smith.[64] Adding this term to the total energy implies the use of a z-component force for each atom given by

$$F_{i,z} = -\frac{q_i}{\varepsilon_o V} M_z \tag{3}$$

The EW3DC method differs from the standard EW3D method only by the presence of this dipole correction. This issue has been discussed in a previous article[42] to model electrostatics efficiently in a 2D periodic system with the standard 3D Ewald method. The functions $S(\mathbf{h})$ and $Q(h)$ are defined using the eqs 4 and 5, respectively

$$S(\mathbf{h}) = \sum_i \sum_a q_{ia} \exp(i\mathbf{h}\cdot\mathbf{r}_{ia}) \tag{4}$$

$$Q(h) = \frac{1}{h^2} \exp\left(-\frac{h^2}{4\alpha^2}\right) \tag{5}$$

where the reciprocal lattice vector $\mathbf{h}$ is defined as $\mathbf{h} = 2\pi(l/L_x\mathbf{u}, m/L_y\mathbf{v}, n/L_z\mathbf{w})$ where $\mathbf{u}$, $\mathbf{v}$, and $\mathbf{w}$ are the reciprocal space basis vectors and l, m, and n take values of 0, ±1, ±2, ···, ±∞. The reciprocal space sum is truncated at an ellipsoidal boundary at the vector $|\mathbf{h}^{max}|$.

Simulations were run in the constant-NVT statistical ensemble using Hoover thermostat[66] with a coupling constant of 0.5 ps. Keeping the cell volume constant is useful for preserving a vacuum zone between periodic images along the z-axis. However, as the inner distance between the closing surfaces cannot change, care was taken for choosing the number of water molecules. For each system, the number of water molecules was adjusted so that the bulk density can be recovered as close as possible to the surfaces.

Methodology. The equations of motion were integrated using the Verlet leapfrog algorithm scheme at $T = 298$ K with a time step equal to 2 fs. The cutoff radius for the Lennard-Jones contribution was fixed to 12 Å, whereas it was equal to 18 Å for the real space of the electrostatic interactions. We also used a reciprocal space cutoff radius of 1.14 Å^{-1}. The configurations were generated using the parallel version of the modified DL_POLY_MD package[67] by using up to 8 processors at a time. The parameters of the long-range electrostatics interactions evaluated Ewald summation technique were calculated in order to satisfy a relative error of 10^{-6}. One simulation run consists of an equilibrium period of 500 ps and an acquisition period of 1 ns.

We have simulated two model systems. In the "clustered" system, 10 alkylferrocene molecules are grafted onto the gold surface close to each other. The remaining surface is grafted with alkyl chains. Thus, the alkyl and alkylferrocene chains are considered as two separated phases in this model system. In the "isolated" system, the 10 alkylferrocene chains are randomly grafted, and alkyl chains are also added to fill the surface. The gold surface is composed of 15 × 16 unit cells, so the dimensions of the simulation box along the x and y axes are 43.2 × 39.9 Å^2. The z dimension is set to 80.0 Å between the two inner gold surfaces. The water and $NaClO_4$ molecules are randomly added in the remaining volume in order to respect a concentration of 1 M for the supportiong electrolyte and an accurate bulk density for water. The number of each molecule type is given in Table 1. Each system has been simulated using two sets of charges to model the neutral and oxidized states of the ferrocene headgroup. This gives four systems, labeled as RAND-Fc and RAND-Fc$^+$ for the neutral and oxidized isolated systems, and CLUS-Fc and CLUS-Fc$^+$ for the neutral and oxidized clustered systems, respectively. Figure 1a displays the two sets of charges used to model the different states of the ferrocene groups. The charges for the Fc systems are part of the force field by Canongia Lopes et al.[59] The atomic charges for the Fc$^+$ systems have been calculated from the density-functional theory (DFT)[68,69] (B3LYP)[70−72] with effective core potential (SD-DALL) Gaussian basis using the Gaussian 03 package[73] and the CHELPG[74] procedure as a grid-based method. Figure 1b shows a snapshot of a typical configuration obtained during the simulation.

TABLE 1: Summary of the Different Parameters for the Simulated Sytems[a]

system	n_{alkFc}	n_{alk}	$n_{ClO_4^-}$	n_{Na^+}	n_{water}	n_{atoms}
RAND-Fc	10	56	62	62	3450	17994
RAND-Fc$^+$	10	56	62	52	3450	17984
CLUS-Fc	10	63	62	62	3450	18218
CLUS-Fc$^+$	10	63	62	52	3450	18208

[a] n_{alk} and n_{alkFc} are the number of grafted alkyl and alkylferrocene molecules, respectively. The number of water molecules n_{water} is adjusted so that the bulk density is respected. To respect the overall zero charge of the system, 10 Na^+ cations are removed in the oxidized systems.

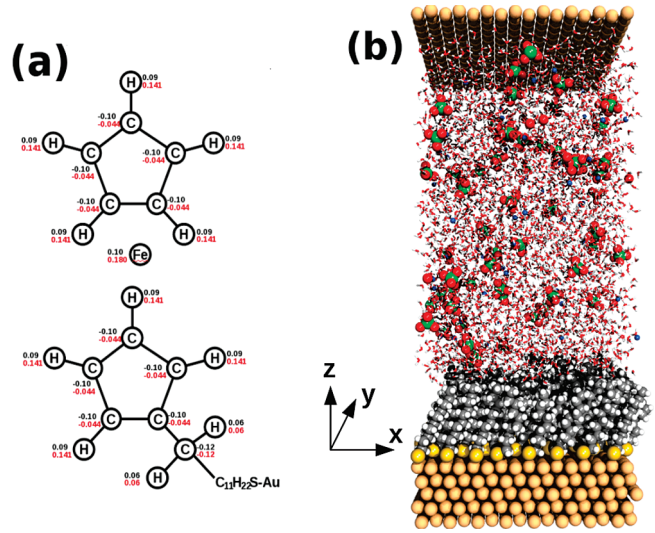

Figure 1. (a) Summary of the atomic charges used in the alkylferrocene (black text) and alkylferrocenium (red text) molecules; (b) snapshot of a configuration for the oxidized clustered system resulting from the production phase.

Results and Discussions

For the random system, the molecular density profiles of the carbon groups in the ferrocenylalkylthiolate chains are shown in Figure 2a along the z-axis normal to the gold surface. The first peak corresponds to S−C bond, whereas the remaining peaks represent the C−C bonds. For the neutral ferrocene moieties, a relatively dense packing geometry of alkylthiols chains is observed. The presence of a doublet pattern is an indication of all-trans structure in the backbone place (the C−C bond takes an alternative sequence of two orientations, nearly parallel and normal, with respect to the surface normal). However, we note that this doublet pattern is less pronounced compared to that of systems with only alkylthiolate chains.[46,75] As concerns the molecular density profiles of Fc$^+$-SAM

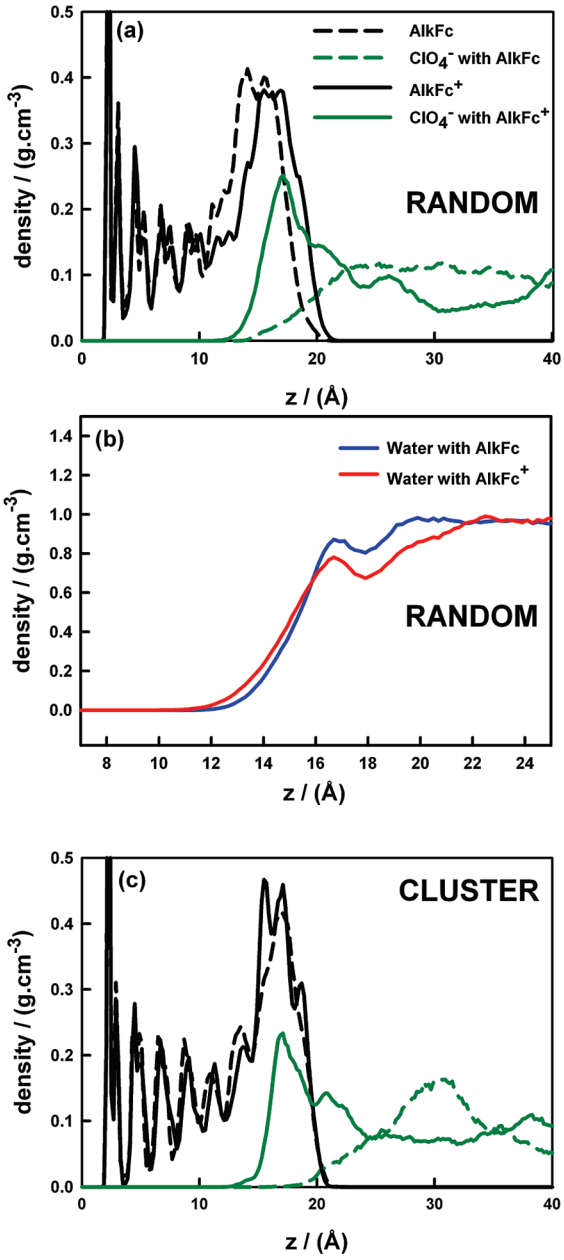

Figure 2. (a) Atomic density profiles of the carbon groups and the perchlorate anions along the *z*-direction in the random system; (b) water molecular density profiles along the z-direction in the random system; (c) atomic density profiles of the carbon groups and the perchlorate anions along the z-direction in the cluster system.

monolayers, the oxidation leads to almost the same doublet pattern for the C−C bonds. A slight shift to a larger distance for the last broader peak corresponding to the ferrocenium cyclopentadiene rings is nevertheless observed. This shift arises from a molecular orientational change in the SAM and indicates a more perpendicular orientation of the cyclopentadiene rings with respect to the surface normal upon oxidation of the ferrocene to ferrocenium. The density profiles of the perchlorate anions along the *z*-direction in the random system are also reported in Figure 2a. As expected, the oxidation of SAMs has a dramatic influence on the profiles of the counterions. Indeed, we observe the emergence of a peak inside the region of the cyclopentadiene rings that shows the incorporation of ClO_4^- into the monolayers. They counterbalance the ferrocenium ions. Various experiments of cyclic voltammetry[13,17,35] and electrochemical quartz crystal microbalance[49,52] have already established that the perchlorate anions strongly complex the terminal ferrocenium cations to form 1:1 ion pairs at the monolayer/solution interface. Furthermore, for a well-packed SAM, the 1:1 contact ion pairing between the oxidized ferrocene and the ClO_4^- at the monolayer/interface is so strong that the monolayer, including the associated anions, behaves as a rigid layer.[52] This is also confirmed by the molecular density profile of the perchlorate anions reported herein.

The density profiles of the water molecules are shown in Figure 2b in the random system. We note that the penetration of the water molecules into the monolayers is increased upon Fc oxidation indicating that the Fc-terminated SAM becomes slightly more hydrophilic. Futhermore, we observe a deficit of water molecules at the rim of the monolayers. This is consistent with experimental studies employing perchloric acid or perchlorate salts as the supporting electrolyte.[27,76] They have stated that ClO_4^- causes the alkanethiol SAMs bearing redox-active terminal groups to be more compact and to contain fewer solvent molecules than other ions such as Cl^- and NO_3^-.[27,76]

To investigate the consequence of the phase state ("isolated" or "clustered") on the oxidation of the ferrocene to ferrocenium, we now focus on the cluster system (Figure 2c). The molecular density profiles of the carbon groups show a less pronounced doublet pattern of the chains compared to that of the random system. This is in excellent agreement with previous results[46] demonstrating that the conformations in the "clustered" state reflect a higher ordering within the cluster structure with a vertical position of the ferrocene moieties. As a result, the surface packing density of the ferrocenylalkylthiolate chains is lower because of the large size of the ferrocene headgroup providing more mobility of the ferrocenylalkylthiolate chains. Another important consideration is that the profile is less affected by the oxidation of the ferrocene to the ferrocenium highlighting that the redox-induced changes seems to be attenuated in the cluster system. Figure 2c also shows the molecular density profiles of the perchlorate anions for the cluster system. As the cluster does not occupy the entire plane, the profile is calculated only for ions located in the *xy* zone defined by the cluster boundary. As in the case of the random system, we observe the emergence of a main peak in the profile of the perchlorate anions after the oxidation of the Fc. It indicates the uptake of the anions by the monolayer upon its oxidation. The propensity of ClO_4^- to form ion pairs with Fc^+ is also illustrated in Figure 3b where a typical snapshot of the cluster system at the monolayer/solution interface is represented after the oxidation of the Fc. The snapshot obtained before the oxidation (Figure 3a) clearly shows any ion pairs formation.

We consider the behavior of the electrostatic potential ϕ across the simulation cell in the random system. ϕ is calculated from the mean charge densities via Poisson's equation

$$\nabla^2\phi = -\frac{\rho}{\varepsilon_0} \tag{6}$$

Applying this equation to the profiles of the mean charge densities $\rho_c(z)$ (Figure 4a) results in a profile of the electrostatic potential along the normal to the surface calculated from

$$\phi(z) - \phi(0) = -\frac{1}{\varepsilon_0}\int_0^{\infty} dz' \int_0^{z'} dz'' \, \rho_c(z'') \tag{7}$$

The potential profiles are shown in Figure 4b. The narrow peaks close to the gold surface result from the packing effects due to the grafting of chains; they are identical for the oxidized and neutral systems. When the ferrocene is oxidized, the partial charges of the ferrocene headgroup are changed. As a conse-

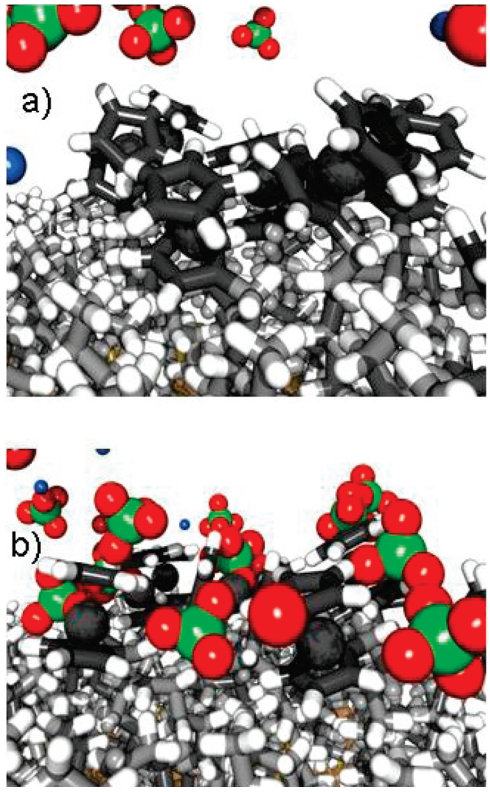

Figure 3. Snapshots of the MD configuration for the cluster system at the monolayer/solution interface (a) before the oxidation of the Fc, (b) after the oxidation of the Fc. The configurations are represented without any water molecules to better highlight the 1:1 ion pairs formation between the Fc^+ and the ClO_4^-.

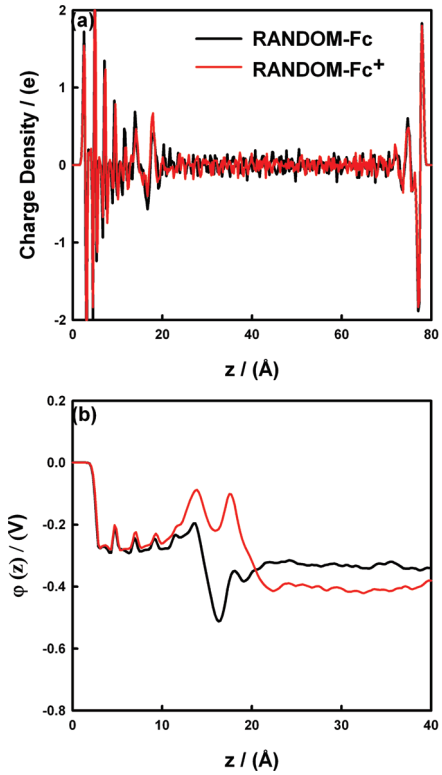

Figure 4. (a) Charge density profiles across the simulation box in the random system; (b) potential profiles across the simulation cell in the random system.

quence, the local electrostatic potential at the region of Fc exhibits significant differences compared to that of the neutral

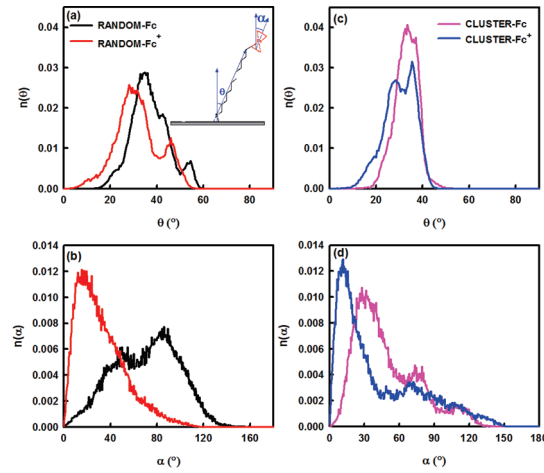

Figure 5. (a) Probability distribution of the tilt angle θ for the ferrocenylalkylthiolate chains in the random system before and after the oxidation of the ferrocene. The inset shows a schematic representation of the tilted ferrocenylalkylthiolate molecule: θ and α are the tilt angles of the molecule and of the ferrocene headgroup with the surface normal, respectively. (b) Probability distribution of the tilt angle α in the random system before and after the oxidation of the ferrocene. (c) Probability distribution of the tilt angle θ for the ferrocenylalkylthiolate chains in the cluster system before and after the oxidation of the ferrocene. (d) Probability distribution of the tilt angle α in the cluster system before and after the oxidation of the ferrocene.

systems. We observe that oxidizing the system leads to an increase of the local electrostatic potential in the region of ion-pairs formation between the perchlorate anion and the ferrocenium cation. This difference in electrostatic potential between the oxidized and neutral forms of the Fc at $z = 16$ Å is positive as expected for an oxidation process. At large z, we check that the electrostatic potential profile is flat as expected for a correct screening of the different partial charges in the system. The electroneutrality is locally verified (see Figure 4a).

We have calculated different angles for the orientation of the ferrocenylalkylthiolate and alkylthiolate chains with respect to the surface in order to provide details of the molecular scale architecture. Both systems are displayed for comparison. The tilt angle θ is defined as the angle between the final backbone atom and the surface normal direction while the tilt angle α is the angle of the ferrocene unit with the surface normal direction as represented in the inset of Figure 5a.

In the random system, the angular distribution of θ of the neutral ferrocenylalkylthiolate chains shows one broad peak (Figure 5a). With regards to the α angle (Figure 5b), the angle distribution is practically uniform in the range of 30°−100°. These results reveal that there is no privileged orientation of chains and that the chain conformations can substantially change in this system in agreement with our previous studies.[44] Actually, the hydrophobic ferrocene groups prefer to interact with the methyl alkyl chains rather than with the hydrophilic interfacial region. For this purpose, two limiting behaviors could be considered. The first one is related only to the tilting of the terminal ferrocene group, whereas the second one concerns rather the tilting of all the ferrocenylalkylthiolate chain. The two limiting behaviors are not equally probable with a large proportion of chains adopting a rather large α configuration because it involves less movement of the neighbor chains.[46]

It appears that the angular distributions obtained for the oxidized ferrocene are quite different from those resulting from the neutral ferrocene moieties. Indeed, we observe a slight shift of the broad peak for the tilt angle θ (Figure 5a) and the

emergence of a well-defined peak at small value of α (Figure 5b). This well-defined peak is directly related to the orientation change for the ferrocene moiety, showing that the ferrocenium cations adopt a vertical position in the SAM. Consistent with the density profile described above, the angular distributions of θ and α clearly evidence the molecular orientational changes in the random system upon oxidation of the Fc groups.

The angular distributions of θ and α in the cluster system are also summarized in Figure 5c,d. A distribution of θ (Figure 5c) with only a unique peak centered at 31° is obtained with the neutral ferrocenylalkylthiolate chain. Concerning the angular distribution of α (Figure 5d) we observe a broad peak located at small value of α. We have previously shown[46] that the corresponding conformations to ferrocene moieties in the "clustered" state rather lead to small values of both θ and α. These results are in line with the steric crowding of the relatively large ferrocene groups leading to a vertical position of the ferrocene moieties in the cluster. Consequently, the average distance of the ferrocene heads from the Au surface is increased and this is probably at the origin of a significant change in long-range electron transfer kinetics. It is thoroughly consistent with the more anodic potential obtained in a number of previous reports[31,32,53] for the oxidation process at high ferrocene coverage. Note that the peak position is probably also affected by the neighboring charge effect.[31,32] When the ferrocenes are clustered, positive charges from the neighboring ferrocenium ions will make the oxidation of ferrocene unfavorable pushing the $E^{\circ\prime}$ to higher potential. After the oxidation of the Fc groups, we observe a slight shift of the peak at lower values for the two angular distributions. In summary, the changes are significantly lower than those obtained in the case of the random system.

A thorough review of the literature indicates that the reorganization of the monolayer was found to be affected by the complexation of the perchlorate by the ferrocenium.[77] Indeed, to facilitate the association of the ferrocenium cations with perchlorate counterions, a stretching to the surface-tethered ferrocenylalkylthiolate was proposed.[77] The observed changes in film thickness were evidenced by spectroscopy.[24,48,49,56,78] Both an untilting of the alkyl chains[24,49] and a more perpendicular orientation of the ferrocene cyclopentadiene rings with respect to the surface normal[48,78] have been proposed. In line with these experimental results, MD simulations indicate that ferrocene oxidation causes a weak decrease of the tilt angle of the alkyl chain with respect to the surface normal and an appreciable change in the orientation of the ferrocene moiety in the random system. The effect arising from the electrostatic repulsion between the positively charged electrode (due to the potential region where the ferrocene is oxidized) and the ferrocenium cation is not considered in this work and can impact the tilt angle of the alkyl chain. However, we assume that this repulsion would have only a moderate effect on the tilt angle especially in the cluster system where the distance between the ferrocene heads and the gold electrode surface is greater.[44] Our results also highlight that the redox-induced change is mainly observed in the random system and it is less pronounced in the cluster system. Such a result could be easily explained by the fact that, initially, the ferrocene headgroup is in a vertical position in the cluster system. As a result, the oxidation of Fc does not induce a significant change in this system.

The formation of self-assembled monolayer depends on the competition among several forces, such as the intrachain, interchain, chain-surface, and chain-bulk interactions, which ultimately determine the molecular orientation near the surface.

TABLE 2: Energy Contributions in kJ mol^{-1} for the Four Studied Systems

contributions	RAND-Fc	RAND-Fc$^+$	CLUS-Fc	CLUS-Fc$^+$
$E_{\text{Fc-Fc}}$	−5.3	9.5	−26.7	21.9
$E_{\text{Fc-Alk}}$	−30.3	−14.2	−26.8	−9.2
$E_{\text{Fc-H}_2\text{O}}$	−46.4	−65.1	−32.8	−68.97
$E_{\text{Fc-ClO}_4^-}$	−1.7	−117.4	−1.7	−136.4
$E_{\text{Fc-Na}^+}$	0.2	12.0	0.3	6.89

We are interested to compare the energy of the interactions involving the ferrocene group as a function of the random and cluster systems before and after the oxidation of Fc. The total interaction energy of the ferrocene groups has been split into five distinct parts: the interactions with other ferrocene groups ($E_{\text{Fc-Fc}}$), with alkyl groups ($E_{\text{Fc-Alk}}$), with water molecules ($E_{\text{Fc-H}_2\text{O}}$), with perchlorate anions ($E_{\text{Fc-ClO}_4^-}$), and with sodium cations ($E_{\text{Fc-Na}^+}$). Each energy contribution sums the Lennard-Jones and electrostatic energy parts.

The average contributions obtained for the two systems before and after the oxidation are reported in Table 2 and are represented in Figure 6. Interestingly, the average contributions in the two types of systems after the oxidation of the ferrocene are very similar, whereas the same contributions are quite different in the two neutral systems. To complete this analysis, we examine in details all kinds of contributions involving the neutral ferrocene moieties. As expected, in the random system the contribution of $E_{\text{Fc-Fc}}$ in the total energy is weak since the separation is large between the ferrocene units. By contrast, in the cluster state, the vertical position due in part to smaller distances between the grafting sites of the ferrocene headgroup increases this Fc−Fc interaction. Since in the random system the ferrocene groups prefer to interact with the methyl alkyl chains rather than with the hydrophilic interfacial region, $E_{\text{Fc-Alk}}$ is higher than that for the second system. Concerning

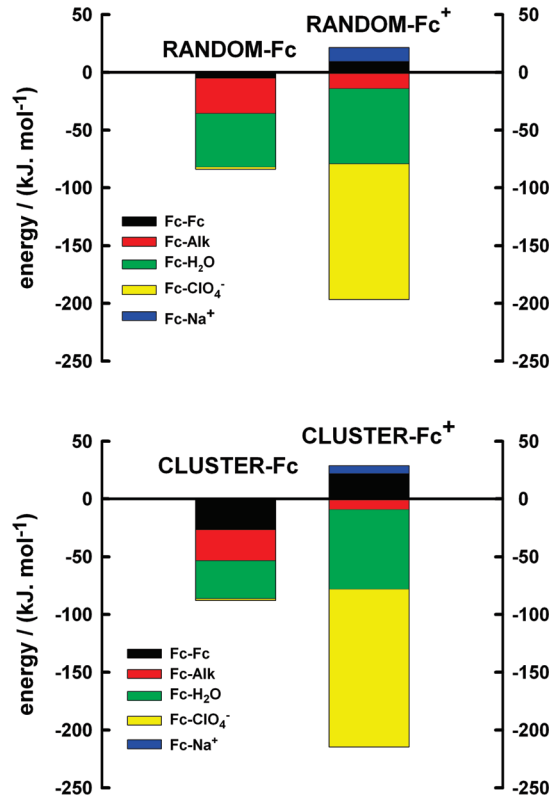

Figure 6. Calculated energy contributions for the random and cluster systems before and after the oxidation of the ferrocene.

the contribution of $E_{Fc\text{-}H_2O}$, we check in the two systems a slight increase of the hydrophilic property of the monolayer after the oxidation of the terminal Fc moiety. As expected, the interactions with the supporting electrolyte are negligible in the neutral systems. Significant differences appear in these contributions after the oxidation of Fc to Fc^+. This observation is perfectly consistent with the redox-induced change resulting mainly from the complexation of perchlorate ions to the surface-immobilized ferroceniums. The Fc-ClO_4^- contribution is 16% higher in the CLUS-Fc^+ system than in the RAND-Fc^+ system. This is due to the high concentration of counterions inside the cluster, which leads to strong ion-pairing. Consequently, the Na^+ cations are more likely to stay far from the ferrocenium groups in the clustered system: $E_{Fc\text{-}Na^+}$ is then 40% smaller in the CLUS-Fc^+ system.

Conclusion

We have reported molecular dynamics simulation of the 12-ferrocenyl-1-dodecanethiol SAMs on gold in 1 M $NaClO_4$, mimicking the conditions of electrochemical experiments by performing simulations including the oxidized form of the ferrocene Fc^+. Two systems have been studied to model dilute and clusterized Fc systems. The computed quantities (density profiles, angular distributions and energetic description) explore the possibility of redox-induced orientation change.

In the random system, the molecular density profiles of the carbon groups indicate a molecular orientational change of the ferrocenium cyclopentadiene rings upon oxidation of the Fc to the Fc^+. In the cluster system, the molecular density profile is less affected by the oxidation highlighting that the redox-induced changes is reduced in this system.

The density profiles of the perchlorate anions along the z-direction in the two systems are also reported. The oxidation of SAMs has a dramatic influence on the density profiles of the perchlorate anions with the emergence of one peak in the region of Fc^+ showing the incorporation of ClO_4^- into the monolayers to counterbalance the ferrocenium ions. A deficit of water molecules at the rim of the monolayer is observed in the density profiles of the water molecules after the oxidation of the terminal Fc to Fc^+ in perfect agreement with experimental results.[27,76]

The combinaison of the angular distributions of θ and α can precisely quantify the conformation of the ferrocenylalkylthiolate chains. These distributions clearly evidence the molecular orientation changes in the random system with a more perpendicular orientation of the cyclopentadiene rings with respect to the surface normal. We also observe that the changes are significantly smaller in the cluster system. In fact, such a result could be easily explained by the fact that in the cluster state, initially, the Fc group is in a vertical position.

These results are confirmed by an energetic study of the Fc group as a function of the system studied (random or cluster systems). In the two types of systems, the contributions become very similar after the oxidation of the Fc to the Fc^+, whereas initially these contributions are quite different. Significant differences appear in the interactions involving the ferrocene and the supporting electrolyte. This result is in line with the redox-induced change resulting principally from the complexation of perchlorate ions to the surface-immobilized ferroceniums.

From this work, we have demonstrated the ability of molecular dynamics simulations to enable better an understanding of the SAM structure. To further understand these electrochemical systems, we plan to use a perturbation method for changing the ferrocenyl groups to the ferrocenium ions. The simulations reported here contribute to a better characterization of the initial and final states of the perturbation process. This technique may lead to a study of the effects that influence the interfacial electron transfer process.

Acknowledgment. This work was granted access to the HPC resources of IDRIS under the allocation 2009-i2009092119 made by GENCI (Grand Equipement National de Calcul Intensif).

References and Notes

(1) Izumi, R.; Hayama, K.; Hayashi, K.; Toko, K. *Chem. Sens.* **2004**, *20*, 50.
(2) Kishimoto, M.; Ikenaga, Y.; Siigi, H.; Nagaoka, T. *Chem. Sens.* **2002**, *18*, 31.
(3) Kim, D.-S.; Park, H.-J.; Park, J.-E.; Shin, J.-K.; Kang, S.-W.; Seo, H.-I.; Lim, G. *Sens. Mater.* **2005**, *17*, 259.
(4) Campuzano, S.; Pedrero, M.; Pingarron, J. *Talanta* **2005**, *66*, 1310.
(5) Kitagawa, K.; Morita, T.; Kimura, S. *Langmuir* **2005**, *21*, 10624.
(6) Chen, J.; Reed, M. A.; Rawlett, A. M.; Tour, J. M. *Science* **1999**, *286*, 1550.
(7) Andres, R. P.; Bein, T.; Dorogi, M.; Feng, S.; Henderson, J. I.; Kubiak, C. P.; Mahoney, W.; Osifchin, R. G.; Reifenberger, R. *Science* **1996**, *272*, 1323.
(8) Ulman, A. *An Introduction of Ultrathin Organic Films: From Langmuir-Blodgett to Self-Assembly Academic*; Academic Press: San Diego, CA, 1991.
(9) Love, J. C.; Estroff, L. A.; Kriebel, J. K.; Nuzzo, R. G.; Whitesides, G. M. *Chem. Rev.* **2005**, *105*, 1103.
(10) Ulman, A. *Chem. Rev.* **1996**, *96*, 1533.
(11) Lee, L. Y. S.; Lennox, R. B. *Phys. Chem. Chem. Phys.* **2007**, *9*, 1013.
(12) Chidsey, C. E. D. *Science* **1991**, *251*, 919.
(13) Chidsey, C. E. D.; Bertozzi, C. R.; Putwinski, T. M.; Mujsce, A. M. *J. Am. Chem. Soc.* **1990**, *112*, 4301.
(14) Uosaki, K.; Sato, Y.; Kita, H. *Electrochim. Acta* **1991**, *7*, 1793.
(15) Uosaki, K.; Sato, Y.; Kita, H. *Langmuir* **1991**, *7*, 1510.
(16) Smalley, J. F.; Feldberg, S. W.; Chidsey, C. E. D.; Linford, M. R.; Newton, M. D.; Liu, Y.-P. *J. Phys. Chem.* **1995**, *99*, 13141.
(17) Creager, S. E.; Rowe, G. K. *Anal. Chim. Acta* **1991**, *246*, 233.
(18) Weber, K.; Hockett, L.; Creager, S. *J. Phys. Chem. B* **1997**, *101*, 8286.
(19) Sumner, J. J.; Weber, K. S.; Hockett, L. A.; Creager, S. E. *J. Phys. Chem. B* **2000**, *104*, 7449.
(20) Chambers, R. C.; Inman, C. E.; Hutchison, J. E. *Langmuir* **2005**, *21*, 4615.
(21) Walczak, M. M.; Popenoe, D. D.; Deinhammer, R. S.; Lamp, B. D.; Chung, C.; Porter, M. D. *Langmuir* **1991**, *7*, 2687.
(22) Voicu, R.; Ellis, T. H.; Ju, H.; Leech, D. *Langmuir* **1999**, *15*, 8170.
(23) Kondo, T.; Takechi, M.; Sato, Y.; Uosaki, K. *J. Electroanal. Chem.* **1995**, *381*, 203.
(24) Ye, S.; Sato, Y.; Uosaki, K. *Langmuir* **1997**, *13*, 3157.
(25) Sabapathy, R. C.; Bhattacharyya, S.; Leavy, M. C.; Cleland, W. E. J.; Hussey, C. L. *Langmuir* **1998**, *14*, 124.
(26) Rowe, G. K.; Creager, S. E. *J. Phys. Chem.* **1998**, *98*, 5500.
(27) Yao, X.; Wang, J.; Zhou, F.; Wang, J.; Tao, N. *J. Phys. Chem. B* **2004**, *108*, 7206.
(28) Quist, F.; Tabard-Cossa, V.; Badia, A. *J. Phys. Chem. B* **2003**, *107*, 10691.
(29) Seo, K.; Jeon, I. C.; Yoo, D. J. *Langmuir* **2004**, *20*, 4147.
(30) Kawaguchi, T.; Tada, K.; Shimazu, K. *J. Electroanal. Chem.* **2003**, *543*, 41.
(31) Auletta, T.; van Veggel, F. C. J. M.; Reinhoudt, D. N. *Langmuir* **2002**, *18*, 1288.
(32) Lee, L. Y. S.; Sutherland, T. C.; Rucareanu, S.; Lennox, R. B. *Langmuir* **2006**, *22*, 4438.
(33) Azzaroni, O.; Yameen, B.; Knoll, W. *Phys. Chem. Chem. Phys.* **2008**, *10*, 7031.
(34) Rowe, G. K.; Creager, S. E. *Langmuir* **1994**, *10*, 1186.
(35) Rowe, G. K.; Creager, S. E. *Langmuir* **1991**, *7*, 2307.
(36) Creager, S. E.; Rowe, G. K. *J. Electroanal. Chem.* **1994**, *370*, 203.
(37) Smith, C. P.; White, H. S. *Anal. Chem.* **1992**, *64*, 2398.
(38) Fawcett, W. R. *J. Electroanal. Chem.* **1994**, *378*, 117.
(39) Brett, D. J. L.; Williams, R.; Wilde, C. P. *J. Electroanal. Chem.* **2002**, *538*, 65.
(40) Beulen, M. W. J.; van Veggel, F. C. J. M.; Reinhoudt, D. N. *Langmuir* **1999**, *18*, 1288.
(41) Calvente, J. J.; Andreu, R.; Molero, M.; Lopez-Perez, G.; Dominguez, M. *J. Phys. Chem. B* **2001**, *105*, 9557.
(42) Goujon, F.; Bonal, C.; Limoges, B.; Malfreyt, P. *Mol. Phys.* **2008**, *106*, 1397.

(43) Goujon, F.; Bonal, C.; Limoges, B.; Malfreyt, P. *J. Phys. Chem. B* **2008**, *112*, 14221.
(44) Goujon, F.; Bonal, C.; Malfreyt, P. *Mol. Simul.* **2009**, *35*, 538–546.
(45) Goujon, F.; Malfreyt, P.; Boutin, A.; Fuchs, A. H. *Mol. Simul.* **2001**, *27*, 99.
(46) Goujon, F.; Bonal, C.; Limoges, B.; Malfreyt, P. *Langmuir* **2009**, *25*, 9164.
(47) Long, H. C. D.; Donohue, J. J.; Buttry, D. A. *Langmuir* **1991**, *7*, 2196.
(48) Viana, A. S.; Jones, A. H.; Abrantes, L.; Kalaji, M. *J. Electroanal. Chem.* **2001**, *500*, 290.
(49) Ye, S.; Sato, T. H. Y.; Shimazu, K.; Uosaki, K. *Phys. Chem. Chem. Phys.* **1999**, *1*, 3653.
(50) Valincius, G.; Niaura, G.; Kazakevicienė, B.; Talaikytė, Z.; Kazamėkaitė, M.; Butkus, E.; Razumas, V. *Langmuir* **2004**, *20*, 6631.
(51) Norman, L. L.; Badia, A. *J. Am. Chem. Soc.* **2009**, *131*, 2328.
(52) Shimazu, K.; Yagi, I.; Sato, Y.; Uosaki, K. *J. Electroanal. Chem.* **1994**, *372*, 117.
(53) Creager, S. E.; Rowe, G. K. *J. Electroanal. Chem.* **1997**, *420*, 291–299.
(54) Ju, H. X.; Leech, D. *Phys. Chem. Chem. Phys.* **1999**, *1*, 1549.
(55) Andreu, R.; Calvente, J. J.; Fawcett, W. R.; Molero, M. *Langmuir* **1997**, *13*, 5189.
(56) Kazakevicien, B.; Valincius, G.; Niaura, G.; Talaikyt, Z.; Kaemkait, M.; Razumas, V.; Plauinatis, D.; Teierskien, A.; Lisauskas, V. *Langmuir* **2007**, *23*, 4965.
(57) Cornell, W. D.; Cieplak, P.; Bayly, C. I.; Gould, I. R.; Merz, K. J.; Ferguson, D. M.; Spellmeyer, D. M.; Fox, T.; Caldwell, J. W.; Kollman, P. *J. Am. Chem. Soc.* **1995**, *117*, 5179.
(58) Rai, B.; Sathish, P.; Malhotra, C. P.; Pradip; Ayappa, K. G. *Langmuir* **2004**, *20*, 3138.
(59) Canongia Lopes, J. N.; do Couto, P. C.; da Piedade, M. E. M. *J. Phys. Chem. A* **2006**, *110*, 13850.
(60) Ryckaert, J. P.; Cicotti, G.; Berendsen, H. J. C. *J. Comput. Phys.* **1977**, *23*, 327.
(61) Abascal, J. L. F.; Vega, C. *J. Chem. Phys.* **2005**, *123*, 234505.
(62) Klähn, M.; Seduraman, A.; Wu, P. *J. Phys. Chem. B* **2008**, *112*, 10989.
(63) Allen, M. P.; Tildesley, D. J. *Computer Simulation of Liquids*; Oxford University Press: New York, 1981.
(64) Smith, E. R. *Proc. R. Soc. London, Ser. A* **1981**, *375*, 475.
(65) Yeh, I.-C.; Berkowitz, M. L. *J. Chem. Phys.* **1999**, *111*, 3155.
(66) Hoover, W. G. *Phys. Rev. A* **1985**, *31*, 1695.
(67) DLPOLY is a parallel molecular dynamics simulation package developed at the Daresbury Laboratory Project for Computer Simulations under the auspices of the EPSRC for the Collaborative Computational Project for Computer Simulation of Condensed Phases (CCP5) and the Advanced Research Computing Group (ARCG) at the Daresbury Laboartory.
(68) Honenberg, P.; Kohn, W. *Phys. Rev. A* **1964**, *136*, 864.
(69) Kohn, W.; Sham, L. *J. Phys. Rev. A* **1965**, *140*, 1133.
(70) Becke, A. D. *Phys. Rev. A* **1988**, *38*, 3098.
(71) Becke, A. D. *J. Chem. Phys.* **1993**, *98*, 5648.
(72) Perdew, J. P.; Wang, Y. *Phys. Rev. E* **1991**, *45*, 13244.
(73) Frisch, M. J.; Trucks, G. W.; Schlegel, H. B.; Scuseria, G. E.; Robb, M. A.; Cheeseman, J. R.; Montgomery, J. A., Jr.; Vreven, T.; Kudin, K. N.; Burant, J. C.; Millam, J. M.; Iyengar, S. S.; Tomasi, J.; Barone, V.; Mennucci, B.; Cossi, M.; Scalmani, G.; Rega, N.; Petersson, G. A.; Nakatsuji, H.; Hada, M.; Ehara, M.; Toyota, K.; Fukuda, R.; Hasegawa, J.; Ishida, M.; Nakajima, T.; Honda, Y.; Kitao, O.; Nakai, H.; Klene, M.; Li, X.; Knox, J. E.; Hratchian, H. P.; Cross, J. B.; Adamo, C.; Jaramillo, J.; Gomperts, R.; Stratmann, R. E.; Yazyev, O.; Austin, A. J.; Cammi, R.; Pomelli, C.; Ochterski, J. W.; Ayala, P. Y.; Morokuma, K.; Voth, G. A.; Salvador, P.; Dannenberg, J. J.; Zakrzewski, V. G.; Dapprich, S.; Daniels, A. D.; Strain, M. C.; Farkas, O.; Malick, D. K.; Rabuck, A. D.; Raghavachari, K.; Foresman, J. B.; Ortiz, J. V.; Cui, Q.; Baboul, A. G.; Clifford, S.; Cioslowski, J.; Stefanov, B. B.; Liu, G.; Liashenko, A.; Piskorz, P.; Komaromi, I.; Martin, R. L.; Fox, D. J.; Keith, T.; Al-Laham, M. A.; Peng, C. Y.; Nanayakkara, A.; Challacombe, M.; Gill, P. M. W.; Johnson, B.; Chen, W.; Wong, M. W.; Gonzalez, C.; Pople, J. A. *Gaussian 03*, revision A.1; Gaussian, Inc.: Wallingford, CT, 2004.
(74) Breneman, C. P.; Wiberg, K. B. *J. Comput. Chem.* **1990**, *11*, 361.
(75) Vemparala, S.; Karki, B. B.; Kalia, R. K.; Nakano, A.; Vashista, P. *J. Chem. Phys.* **2004**, *121*, 4323.
(76) Long, H. C. D.; Buttry, D. A. *Langmuir* **1990**, *6*, 1319.
(77) Cruanes, M. T.; Drickamer, H. G.; Faulkner, L. R. *Langmuir* **1995**, *11*, 4089.
(78) Popenoe, D. D.; Deinhammer, R. S.; Porter, M. D. *Langmuir* **1992**, *8*, 2521.

JP911467X